Pt(IV) pro-drugs with an axial HDAC inhibitor demonstrate multimodal mechanisms involving DNA damage and apoptosis independent of cisplatin resistance in A2780/A2780cis cells

Awatif Rashed Z. Almotairy[a,b], Diego Montagner[c], Liam Morrison[d], Michael Devereux[b], Orla Howe[b,*], Andrea Erxleben[a,**]

[a] *School of Chemistry, National University of Ireland, Galway, Ireland*
[b] *School of Biological & Health Sciences, Technological University Dublin, City Campus, Dublin, Ireland*
[c] *Department of Chemistry, Maynooth University, Maynooth, Ireland*
[d] *Earth and Ocean Sciences, School of Natural Sciences and Ryan Institute, National University of Ireland, Galway, Ireland*

ARTICLE INFO

ABSTRACT

Epigenetic agents such as histone deacetylase (HDAC) inhibitors are widely investigated for use in combined anticancer therapy and the co-administration of Pt drugs with HDAC inhibitors has shown promise for the treatment of resistant cancers. Coordination of an HDAC inhibitor to an axial position of a Pt(IV) derivative of cisplatin allows the combination of the epigenetic drug and the Pt chemotherapeutic into a single molecule. In this work we carry out mechanistic studies on the known Pt(IV) complex *cis,cis,trans*-[Pt(NH$_3$)$_2$Cl$_2$(PBA)$_2$] (**B**) with the HDAC inhibitor 4-phenylbutyrate (PBA) and its derivatives *cis,cis,trans*-[Pt(NH$_3$)$_2$Cl$_2$(PBA)(OH)] (**A**), *cis,cis,trans*-[Pt(NH$_3$)$_2$Cl$_2$(PBA)(Bz)] (**C**), and *cis,cis,trans*-[Pt(NH$_3$)$_2$Cl$_2$(PBA)(Suc)] (**D**) (Bz = benzoate, Suc = succinate). The comparison of the cytotoxicity, effect on HDAC activity, reactive oxygen species (ROS) generation, γ-H2AX (histone 2A-family member X) foci generation and induction of apoptosis in cisplatin-sensitive and cisplatin-resistant ovarian cancer cells shows that **A – C** exhibit multimodal mechanisms involving DNA damage and apoptosis independent of cisplatin resistance.

1. Introduction

Cisplatin (*cis*-[Pt(NH$_3$)$_2$Cl$_2$]) has been used as a chemotherapeutic cancer drug since 1978, specifically in the treatment of testicular, head and neck, bladder and ovarian carcinomas [1]. The generally accepted mode of action of cisplatin involves covalent binding of the *cis*-Pt(NH$_3$)$_2$$^{2+}$ entity to adjacent guanine bases in DNA following loss of the chlorido leaving group ligands. The formation of these DNA lesions triggers the DNA damage response by activating or silencing various genes. If the damage is beyond repair, mitochondrial apoptosis is initiated [2,3].

Inherent and acquired resistance towards platinum drugs presents a major clinical challenge and a significant limitation of platinum-based chemotherapy [4]. Cisplatin resistance is the consequence of genetic and epigenetic changes that lead to decreased cellular uptake, increased cellular efflux, detoxification due to increased glutathione or thioredoxin levels, enhanced DNA repair, enhanced DNA damage tolerance

and late apoptotic response [5]. The main types of epigenetic alterations in general are DNA methylation and histone methylation or acetylation [6]. Histone acetylation and deacetylation regulate gene expression by opening (acetylation) and closing (deacetylation) the chromatin [7]. Histone acetylation has a critical regulatory function in DNA repair and recent studies suggest that it plays a role in the development of drug resistance [4]. Histone acetylation and deacetylation are catalyzed by histone acetyltransferase (HAT) and histone deacetylase (HDAC) respectively.

The combination of epigenetic drugs with conventional chemotherapy shows significant promise as a strategy for the treatment of resistant cancers [8]. Several HDAC inhibitors (HDACis) have entered clinical trials [9,10] and the first HDACi was approved by the FDA in 2006 [11]. Several studies have shown that the co-administration of cisplatin with an HDACi leads to enhanced therapeutic efficacies [12–14]. Belinostat in combination with cisplatin reverses resistance in Pt-resistant lung cancer cells [15]. Trichostatin A has an additive effect

---

with oxaliplatin in gastric tumor cells [16]. Pt-resistant ovarian cancer cells are sensitized to cisplatin-mediated cell death when pre-treated with HDAC and methylation inhibitors [17].

While different pharmacokinetics can be a problem in co-administration, coordination of the HDACi to the Pt centre ensures the simultaneous delivery of both drugs. Marmion and coworkers developed Pt(II) complexes in which a functionalized HDAC inhibitor ligand is coordinated to the *trans*-Pt(NH$_3$)(py)$^{2+}$, *trans*-Pt(py)$_2^{2+}$ (py = pyridine) [18] or *cis*-Pt(NH$_3$)$_2^{2+}$ entity [19–21]. Kasparkova et al. reported a photoactivatable Pt(IV) complex of the HDAC inhibitor suberoyl-bis-hydroxamic acid [22]. Gibson and coworkers and Brabec and coworkers attached the HDACis 4-phenylbutyrate (PBA) and valproate (VPA) to the axial positions of Pt(IV) derivatives of cisplatin, oxaliplatin and [Pt(1S,2Sdiaminocyclohexane)(5,6-dimethyl-1,10-phenanthroline)]$^{2+}$ [23–27]. Pt(IV) complexes are pro-drugs that release the active Pt(II) drug and the axial ligands on intracellular reduction. The bis-PBA complex *cis,cis,trans*-[Pt(NH$_3$)$_2$Cl$_2$(PBA)$_2$] showed an up to 100-fold higher cytotoxicity than cisplatin and significant HDAC inhibition activity suggesting a synergism between Pt and PBA [27]. The Pt(IV) complex *cis,cis,trans*-[Pt(NH$_3$)$_2$Cl$_2$(VPA)$_2$] with the HDACi valproate was studied by Osella and coworkers [28], Shen and coworkers [29] and Gibson and coworkers [27]. Very recently, the same researchers reported a triple-action Pt(IV) complex containing PBA and a second epigenetically acting ligand, octanoate [24,30]. As part of our own work we have recently reported Pt(IV) derivatives of carboplatin with an axial PBA ligand and a second biologically inactive carboxylate ligand to modify the lipophilicity [31].

We compare here the DNA damage, reactive oxygen species (ROS) generation, HDAC activity and induction of apoptosis in cisplatin-sensitive A2780 and cisplatin-resistant A2780cis cells on treatment with the known Pt(IV) complex *cis,cis,trans*-[Pt(NH$_3$)$_2$Cl$_2$(PBA)$_2$] and its derivatives *cis,cis,trans*-[Pt(NH$_3$)$_2$Cl$_2$(PBA)(OH)], *cis,cis,trans*-[Pt(NH$_3$)$_2$Cl$_2$(PBA)(Bz)], and *cis,cis,trans*-[Pt(NH$_3$)$_2$Cl$_2$(PBA)(Suc)] (Bz = benzoate, Suc = succinate) in order to provide more insight into the ability of Pt(IV) PBA pro-drugs to overcome cisplatin resistance in ovarian cancer cells.

2. Experimental

2.1. Syntheses

The syntheses of the Pt(IV) complexes is described in the Supplementary Material.

2.2. Measurements and instrumentation

^{1}H and ^{195}Pt nuclear magnetic resonance (NMR) spectra were recorded with a Varian 500 AR spectrometer. Chemical shifts are given in parts per million (ppm) with tetramethylsilane as the reference (δ (^{1}H NMR) = 0 ppm). Coupling constants (*J*) are given in Hertz (Hz). ^{195}Pt NMR spectra were acquired in dimethylformamide (DMF) with an inserted tube containing D$_2$O. K$_2$PtCl$_6$ in D$_2$O was used as an external reference. Mass spectra were obtained with a Waters LCT Premiere XE with electron spray ionization (ESI) and time of flight mass analyzer. Elemental analyses (carbon, nitrogen and hydrogen) were carried out with a PerkinElmer 2400 series II analyzer. Pt concentrations were measured by inductively coupled plasma mass spectrometry (ICP-MS, ELAN DRCe, PerkinElmer, Waltham, USA) in a class 1000 cleanroom [32–35]. The calibration curve was obtained using known concentrations of platinum standard solutions (0–50 μM).

2.3. Stability studies

Complexes **A** and **C** were dissolved in 0.5 mL dimethylformamide and diluted with 0.5 mL acetonitrile and 3 mL physiological saline (0.9% NaCl) to a final concentration of 6 and 4 mM, respectively. The samples were kept at 37 °C for 72 h and analyzed at regular intervals by

high-performance liquid chromatography (HPLC; Agilent 1200, Phenomenex Luna C18 column, 5 μm, 100 Å, 250 mm × 4.60 mm i.d.). The mobile phase was 70:30 acetonitrile (1% trifluoroacetic acid): water (1% trifluoroacetic acid).

2.4. Monitoring of the reduction of the Pt(IV) complexes by HPLC

The reduction of complexes **A** and **C** was monitored using an Agilent 1200 series diode array detector analytical HPLC instrument. The compounds were dissolved in 0.5 mL dimethylformamide, added to a 7 mM solution of ascorbic acid in 4 mM 4-(2-hydroxyethyl)piperazine-1-ethanesulfonic acid (HEPES) buffer (pH 7) and diluted with acetonitrile to a final concentration of 0.5 mM. The reduction was monitored at 37 °C until completion. The samples were analyzed using a Phenomenex Luna C18 column (5 μm, 100 Å, 250 mm × 4.60 mm i.d.). The mobile phase was 90: 10 acetonitrile (1% trifluoroacetic acid): water (1% trifluoroacetic acid). The flow rate was 1.0 mL min^{-1} and the fractions were detected at 254 nm.

2.5. Determination of lipophilicity

Octanol-water partition coefficients (log$P_{o/w}$) of the Pt(IV) compounds were determined by the shake flask method (Test No. 107: Partition Coefficient (n-Octanol/Water): Shake Flask Method; Organisation for Economic Co-operation and Development: Paris (1995)). All experiments were done in duplicate. The respective Pt(IV) complex was mixed with 0.9% NaCl (*w/v*) in ultrapure water that was presaturated with n-octanol for 3 d. All solutions were sonicated and filtered to remove undissolved Pt(IV) compound. The initial Pt concentrations were measured by ICP-MS as described above. Subsequently, the Pt(IV) solution was added to an equal volume of n-octanol that was presaturated with 0.9% NaCl (*w/v*) in ultrapure water containing 1% HNO$_3$. The heterogeneous mixture was shaken vigorously for 1 h before centrifuging at 4400 rpm for 1 h to achieve phase separation. The final Pt concentration in the aqueous phase was measured again by ICP-MS. Log$P_{o/w}$ values were calculated as the ratio of Pt concentrations in the organic and aqueous phases.

2.6. Experiments with cultured human cells

The tested compounds (**A – D**) were dissolved in dimethyl sulfoxide (DMSO, Merck, Germany) before the start of the experiment. The final concentration of DMSO was ≤0.3%. A2780 and A2780cis cells were obtained commercially from European Collection of Authenticated Cell Cultures (ECACC) (Public Health England, UK). Cells were grown in Roswell Park Memorial Institute (RPMI - 1640) medium (Sigma, Ireland) supplemented with 12% Fetal Bovine Serum (Sigma, Ireland) and 5% L-glutamine (Sigma, Ireland) and incubated at 37 °C in 5% CO$_2$. A sub-lethal dose of 1 μM cisplatin was added to A2780cis cells to maintain cisplatin resistance. Stock cells were grown to 80–90% confluence and were then trypsinised to generate a cell suspension for experimental use.

2.7. Cell viability

Cellular viability was evaluated by the MTT (3-(4,5-dimethylthiazol-2-yl)-2,5-diphenyltetrazolium bromide, Sigma, Ireland) assay which is a colorimetric assay that measures the metabolic activity of cells [36]. The ovarian adenocarcinoma cell lines were plated in 96-well plates with a total number of 1 × 10^4 cells/well and 8 × 10^3 cells/well for 24 and 48 h, respectively for each cell line, and the plates were incubated at 37 °C for 24 h for attachment and growth. Cells were then treated with different concentrations of the test compounds (2.5 μM – 200 μM) in triplicate and a solvent control (0.3% DMSO) for 24 and 48 h timepoints. The cell culture medium and test drug was discarded from the plate wells and 100 μL of a solution of MTT (5 mg / mL) was

added to each well. The cells were incubated for 3 h and washed three times with sterilised PBS. 100 μL of DMSO was added to each well and plates were shaken gently for 15 min to dissolve the coloured formazan crystals formed by cellular nicotinamide adenine dinucleotide phosphate (NADPH) dependent oxidoreductase enzymes. The absorbance at 595 nm of each well was measured using a microplate reader and a 1420 Multilabel Counter Victor3V spectrophotometer (PerkinElmer, USA). All MTT assays were performed in triplicate at three independent times with six replicate wells for each test compound. For statistical analysis, the mean and standard deviation was calculated using Microsoft® Excel (Microsoft Corporation, USA). The calculations of the IC_{50} concentrations for each cell line, timepoint, complex and control was performed using the statistical package GraphPad Prism (Ver. 6.0) (GraphPad, USA). The IC_{50} value is the concentration of the test compounds that reduces the cellular viability by 50%.

2.8. Reactive oxygen species (ROS) assay

The induction of intracellular oxidative stress in A2780 and A2780cis cells was measured using a 2′,7′-dichlorofluorescein diacetate (DCFH-DA) dye which produces fluorescence on the production of reactive oxygen species. Briefly, cells were seeded into 96-well plates at a density of 1×10^4 cells/well and were incubated for 24 h at 37 °C. The medium was removed and 100 μL of a 20 μM DCFH-DA solution in PBS was added to each well and incubated at 37 °C and 5% CO_2 for 60 min in darkness. Cells were washed twice with 100 μL PBS and then treated with 100 μL of 10 μM H_2O_2 in PBS (positive control), with PBS alone (untreated control) and a concentration range of 0.47–60 μM of each test compound. The fluorescence was measured at different time intervals between 15 and 120 min. ROS levels were determined by measuring the fluorescence of oxidized DCFH-DA using a spectramax M3 multiplate reader with excitation at 485 nm and emission at 530 nm. Three independent experiments were done with six replicate wells used for all test compounds, positive control and untreated control.

2.9. Cellular uptake

1×10^6 A2780 cells were seeded in T25 cm^2 flasks in growth medium (5 mL). After overnight incubation the medium was replaced and the cells were treated with IC_{50} concentrations of the tested compounds for 24 h. The cells were washed twice with cold PBS, harvested by trypsinization and counted using a hemocytometer. The cells were vortexed vigorously, frozen at −80 °C, treated with 200 μL of highly pure nitric acid (Trace Metal Grade, 67–69%, Fisher, UK) and transferred into microwave tubes. The tubes were heated at 80 °C in order to digest the cells. After cooling, the samples were diluted with ultrapure water to a final concentration of 1% HNO_3. Each mineralized sample was filtered and the platinum content was analyzed by ICP-MS as described above.

2.10. Platination of cellular DNA

A2780 cells (0.8×10^6) were seeded in 9 cm^2 6-well culture plates in 5 mL of RPMI1640 cell culture medium. After overnight incubation, the medium was replaced, and the cells were treated with IC_{50} concentrations of the tested compounds for 24 h. The cells were washed twice with cold PBS, harvested by trypsinization and counted using a hemocytometer. The cells were stored at −80 °C until analysis. The DNA was extracted and purified by using a cell lysis buffer (2.5% Triton X-100, 100 mM Tris-HCl pH 8, 10 mM ethylenediaminetetraacetate, 2% sodium dodecyl sulfate, 200 mM NaCl, 200 μg mL^{-1} proteinase K) and incubated for 2 h at 56 °C. 6 μL of RNAse A solution (0.4 mg mL^{-1}) was added and samples were incubated at room temperature for 1 h. 1000 μL of 2-propanol was added to each sample in order to precipitate the DNA. The samples were stored overnight at −20 °C. The DNA was

isolated by centrifugation at 18000 ×g for 30 min at 4 °C. Then the DNA pellet was washed with 70% ethanol. The DNA was dissolved in 200 μL of nuclease-free water and the DNA concentration was determined with a MaestroNano spectrophotometer. The samples were stored at −20 °C until analysis. The DNA samples were dried using a freeze dryer and 300 μL of high purity concentrated HNO_3 was added to all samples. The DNA samples were transferred to borosilicate glass microwave tubes. After heating at 80 °C for 2 h to digest the samples, they were diluted with 1% HNO_3 in ultrapure water. The samples were filtered and analyzed by ICP-MS as described above.

### 2.11. Determination of DNA double-strand breaks (DSBs)

The occurrence of DSBs in A2780 and A2780cis cells was quantified by using immunodetection of γ-H2AX (histone 2A-family member X) foci by flow cytometry. Cells were seeded at different densities (1×10^4 cells/well and 8×10^3 cells/well for 24 and 48 h, respectively) and incubated at 37 °C in a humidified, 5% CO_2 atmosphere for 24 h. The cells were exposed to IC_{50} concentrations of the Pt(IV) complexes, cisplatin and PBA over the two incubation times, 24 h and 48 h. Then, the culture medium was removed and the cells were washed with 2 × 4 mL PBS. The cells were harvested and fixed in 200 μL 2% (v/v) paraformaldehyde in PBS for 10 min at room temperature. The solution was removed and 1 mL of cold 95% ethanol was added to fix the cells which were then stored at 4 °C overnight. The ethanol was removed after centrifugation at 800 ×g for 5 min and cells were washed once with PBS and resuspended in 1 mL of 0.25% (v/v) Triton X-100 in PBS for 5 min at room temperature to permeabilise the cells. This was removed and cells were resuspended in 500 μL of blocking solution (PBS containing 4% fetal bovine serum (FBS)) for 30 min at room temperature. The primary antibody (Anti-phospho-histone H2A.X (ser139) antibody, clone JBW301, Mouse, Millipore) was diluted 1:800 with blocking solution and was added to each sample and incubated overnight at 4 °C. The samples were washed with 500 μL of blocking solution and the secondary antibody (Alexa Fluor 488 goat anti-mouse immunoglobulin G (IgG, Invitrogen) was added to the samples for 1 h in the dark. Samples were washed with 500 μL PBS before analysis. The BD Accuri C6 (BD Biosciences, USA) flow cytometer was used to detect foci formation in cells staining positive for γ-H2AX fluorescence and was measured at excitation 495 nm and emission 519 nm. At least three independent experiments were conducted for 1×10^4 cells per analysis.

2.12. Immunodetection of γ-H2AX foci with confocal microscopy

Fixed cells were stained with γ-H2AX and propidium iodide as described above. 100 μL of cells were aliquoted and deposited on glass slides by cytospin centrifugation at 1200 rpm for 15 min. Samples were dried quickly at room temperature for 30 min. Cover slips (0.085–0.13 mm thick) were mounted on the slides by using mounting medium and sealed with clear nail varnish. The LSM© 510 Meta Confocal Microscope (Zeiss, Germany) was used to capture images. The images were analyzed using ImageJ software. All images were taken at 63× magnification with both argon and helium-neon lasers simultaneously scanning into its four component channels; green (γ-H2AX foci), red (propidium iodide), merged and brightfield.

2.13. Apoptosis

The induction of apoptosis in A2780 and A2780cis cells was quantified by flow cytometry using annexin V FITC conjugate (BD Pharmingen™, UK) and propidium iodide (BD Pharmingen™, UK) staining. Both cell lines were seeded into T25 flasks at different densities for two different incubation times; 1×10^4 cells/well for 24 h and 8×10^3 cells/well for 48 h incubation. After 24 h new medium was added and the cells were incubated with IC_{50} doses of the test and reference compounds at 37 °C in a humidified, 5% CO_2 atmosphere for 24
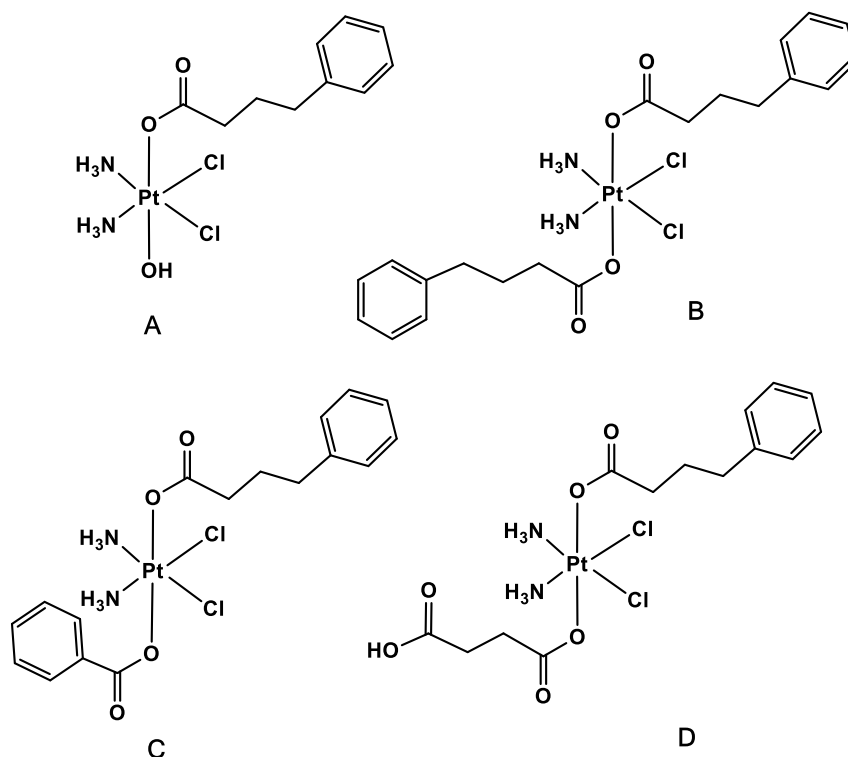
Scheme 1. Chemical structures of complexes **A – D**.

and 48 h. The cells were trypsinised, harvested and centrifuged (400 ×*g* for 6 min). The cells were washed twice with cold PBS followed by 1× binding buffer (2 ×). The cells were resuspended in 1× binding buffer at a concentration of 1×10^6 cells/mL and stained with 5 μL of Annexin V FITC for 15 min. Then 5 μL propidium iodide was added and incubated for 15 mins in the dark. 400 μL of 1× binding buffer was then added and each sample was analyzed by flow cytometry. At least three independent experiments were conducted for 1×10^4 cells per analysis.

2.14. HDAC activity/inhibition direct assay

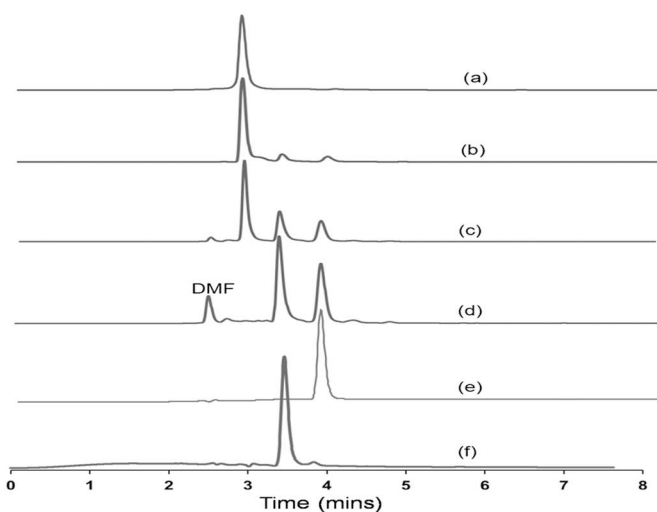Histone deacetylase activity/inhibition was determined using the

Fig. 1. HPLC chromatograms of the reaction of **C** with 10 eq. ascorbic acid at 37 ˚C and pH 7. (a) $t = 0$, (b) 3 h, (c) 9 h, (d) 20 h, (e) the free ligand PBA and (f) the free ligand Bz.

EpiQuik™ HDAC Activity/Inhibition Direct Assay Kit (Colorimetric; Farmingdale, NY). Briefly, A2780 and A2780cis cells were seeded (1×10^6) in T25 cm^2 flasks in growth medium. Cells were treated for 24 h with IC$_{50}$ concentrations of the tested compounds and then processed according to the EpiGentek manufacturer's instructions. The measurement of HDAC activity was done in nuclear extracts according to the manufacturer instructions of a Nuclear Extraction Kit (Nucleic Acid-Free; EpiGentek, Farmingdale, NY). The absorbance was read on a spectraMax M3 multiplate reader at 450 nm within 2–15 min.

3. Results and discussion

3.1. Synthesis and characterization of the complexes

The chemical structures of the Pt(IV) complexes investigated in this study are shown in Scheme 1. The monosubstituted complex *cis,cis,-trans*-[Pt(NH$_3$)$_2$Cl$_2$(PBA)(OH)] (**A**) was synthesized by reacting *cis,cis,-trans*-[Pt(NH$_3$)$_2$Cl$_2$(OH)$_2$] with 0.8 equivalents of the activated NHS-ester of PBA in dimethylsulfoxide at 70 ˚C for 48 h (Scheme S1, Supplementary Material). Reaction of **A** with benzoic and succinic anhydride in dimethylformamide gave the unsymmetric complexes *cis,cis,-trans*-[Pt(NH$_3$)$_2$Cl$_2$(PBA)(Bz)] (**C**) and *cis,cis,trans*-[Pt(NH$_3$)$_2$Cl$_2$(PBA)(Suc)] (**D**). Benzoate and succinate were attached to the second axial position in order to vary the lipophilicity. The bis-substituted complex *cis,cis,trans*-[Pt(NH$_3$)$_2$Cl$_2$(PBA)$_2$] (**B**) was previously synthesized by Gibson and coworkers [27]. The purity and composition of the complexes were confirmed by elemental analysis, HPLC, electrospray ionization mass spectrometry, and ^{1}H and ^{195}Pt NMR spectroscopy.

The log $P_{o/w}$ values, determined using the shake-flask method, were found to be −0.12 ± 0.05 (**A**), 0.16 ± 0.07 (**B**), 0.08 ± 0.02 (**C**) and − 0.14 ± 0.08 (**D**) and demonstrate that the complexes follow the expected order of lipophilicity of **B** > **C** > **A** > **D**.

HPLC analysis of two representative examples of the complexes (**A** and **C**) confirmed that the Pt(IV) prodrugs are stable in physiological saline (0.9% NaCl) at 37 ˚C for at least 72 h (Fig. S1). As Pt(IV) prodrugs require activation by biological reducing agents, the reduction of

the monosubstituted complex (**A**) and of a representative biscarboxylated complex (**C**) was monitored under physiological conditions (37 °C, pH 7) in the presence of ascorbic acid using HPLC (Figs. 1 and S2). The chromatograms show the release of the axial PBA ligand that accompanies the conversion of the octahedral Pt(IV) complexes to square-planar cisplatin. In the case of **C** both, free PBA and free benzoate were identified in the chromatograms. **A** and **C** were completely reduced after 48 and 20 h, respectively. The reduction kinetics of Pt(IV) complexes depend on the nature of the axial ligands, the equatorial ligands and the reducing agent [37]. Complexes with an axial hydroxido ligand are usually reduced faster by ascorbate than bis-carboxylated complexes, as the OH group can act as a bridging ligand and facilitate the electron transfer *via* an inner-sphere mechanism [38]. In the case of complexes of type *cis,cis,trans*-[Pt(NH$_3$)$_2$Cl$_2$L$_2$] with two equatorial chlorido ligands, however, the rate of reduction by ascorbate often correlates with the reduction potential; L = OH ($\sim$ -900 mV) < L = RCOO$^-$ ($\sim$ -600 mV) [1,39] and the faster reduction kinetics of **C** compared to **A** are consistent with this.

3.2. Cytotoxicity

The cytotoxic activities of the complexes were evaluated in two human ovarian carcinoma cells lines, cisplatin-sensitive A2780 and cisplatin-resistant A2780cis. These isogenic cell lines were selected on the basis of their matched genetic background which reduces variability in drug response studies [40]. Chemoresistance has been associated with epigenetic modifications including histone modifications, and the A2780 and A2780cis matched pair of cells is widely used in the study of HDACis [41–43].

The cytotoxicity was determined after incubation for 24 and 48 h using the tetrazolium based MTT colorimetric assay. For comparison purposes, the cytotoxicities of cisplatin and of the uncoordinated HDACi PBA were assessed under the same experimental conditions. IC$_{50}$ values were calculated from the growth inhibition curves and are shown in Table 1. The Pt(IV) complexes displayed dose- and time-dependent cytotoxicities. The IC$_{50}$ values of **A** – **C** are in the low micromolar range, while **D** is only modestly active. In the A2780 cell line, the cytotoxic activities follow the order **C** > > **B** ~ **A** > cisplatin > > **D**. **A** – **D** exhibit similar activities in cisplatin-sensitive and -resistant cells with resistance factors close to 1. The IC$_{50}$ values of the most effective complex **C** were 16- and 37-fold lower than those of cisplatin in the two cell lines (48 h incubation). A comparison of the IC$_{50}$ values at the 24 h and 48 h timepoints shows a decrease by a factor of 4.9–3.3 for the PBA complexes on prolonged exposure compared to a factor of about 2 for cisplatin. The delayed cytotoxicity of the Pt(IV) complexes can be attributed to the requirement for intracellular activation. The fact that the largest reduction in IC$_{50}$ (4.9-fold) is observed for **A** correlates with the slow reduction kinetics of the monocarboxylated complex (complete reduction within 48 h (**A**) *vs.* 20 h (**C**)). In agreement with the literature [27], free PBA elicited no cytotoxicity at

micromolar concentrations. At physiological pH, the carboxyl group is deprotonated so that the IC$_{50}$ value of PBA of > 200 µM may be a consequence of the hampered cellular uptake of its negatively charged form. It has been pointed out in the literature that Pt(IV) PBA complexes are not only pro-drugs of the Pt(II) agent but also present pro-drugs for PBA and this can involve synergistic accumulation [27].

3.3. Cellular uptake and DNA platination

Fig. 2a shows the Pt content in A2780 cells after exposure to IC$_{50}$ doses of cisplatin and complexes **A** – **D** for 24 h. Except for **D**, the Pt(IV) complexes accumulate more efficiently than cisplatin in cells. The poor cellular uptake of **D** can explain the low cytotoxicity of this complex and may be attributed to the hydrophilic succinate ligand which would be negatively charged at pH 7.4. For **A** – **C**, however, the uptake (**B** < **C** < **A**) does not follow the order of increasing lipophilicity (**A** < **C** < **B**) which has also been reported for other Pt(IV) complexes [27,44,45].

As the binding to nuclear DNA is considered to be a crucial event in the cytotoxic action of platinum drugs, the Pt contents of the DNA from treated cells were also determined. A2780 cells were exposed to IC$_{50}$ doses of **A** – **D** and cisplatin for 24 h and after extraction of the DNA the Pt concentration was measured by ICP-MS. The results, expressed as ng Pt per µg of DNA are shown in Fig. 2b. The Pt(IV) complexes gave higher levels of DNA platination than cisplatin, except for **D** that does not enter the cell effectively. It can be assumed that the cellular uptake and reduction kinetics are important for the DNA platination levels after 24 h incubation. The DNA platination in cells treated with **A** and **C** is coherent with this, while the high platination levels observed for complex **B** are somewhat surprising given its relatively low cellular accumulation. It might be speculated that the low cellular uptake is compensated by the strong HDAC inhibitory activity of the complex (see below) that can lead to a greater accessibility of the DNA by keeping the chromatin structure open [6]. The IC$_{50}$ values at the 48 h timepoint (**C** > > **B**, **A** > cisplatin > **D**) correlate with the Pt content in the DNA (**C** > **A** > **B** > cisplatin > **D**). However, at the 24 h timepoint, **A** and **B** have higher IC$_{50}$ values than cisplatin despite their higher DNA platination levels. Apparently, the Pt(IV) complexes take longer to exert their cytotoxicity.

3.4. Cellular reactive oxygen species production

The induction of cellular reactive oxygen species (ROS) production by Pt drugs has been discussed in the literature [46]. Kaluderovic et al. reported enhanced cellular ROS levels in cells treated with tetrachlorido Pt(IV) complexes [47]. The redox and mitochondrial stability can be stressed by treatment with cisplatin due to ROS production [48,49]. We therefore investigated the generation of ROS in A2780 and A2780cis cells after incubation with **A** – **D**, cisplatin and PBA. ROS levels were monitored over a 2 h period using 2′,7′-dichlorofluorescein

Table 1

IC$_{50}$ values of Pt(IV) complexes **A** – **D**, cisplatin and free ligand PBA in A2780 and A2780cis cells determined by the MTT test.

	IC$_{50}$ (µM) $\pm$ S.D.[a]				R.F.[b]	
	A2 780		A2780cis			
	24 h	48 h	24 h	48 h	24 h	48 h
A	24.2 $\pm$ 7.1	4.93 $\pm$ 0.19	35.6 $\pm$ 11.6	6.3 $\pm$ 2.1	1.5	1.3
B	18.4 $\pm$ 4.3	4.6 $\pm$ 1.3	14.2 $\pm$ 2.2	5.1 $\pm$ 1.1	0.8	1.1
C	1.8 $\pm$ 0.1	0.51 $\pm$ 0.16	3.1 $\pm$ 1.4	0.71 $\pm$ 0.36	1.7	1.4
D	124.1 $\pm$ 26.9	38.1 $\pm$ 8.5	149.4 $\pm$ 36.8	43.2 $\pm$ 6.5	1.2	1.1
cisplatin	16.4 $\pm$ 5.2	8.3 $\pm$ 2.4	55.4 $\pm$ 14.1	26.5 $\pm$ 4.7	3.4	3.2
PBA	> 200	> 200	> 200	> 200	–	–

[a] All MTT assays were performed in triplicate at three independent times with six replicate wells for each test compound.

[b] R.F. = resistance factor; ratio of IC$_{50}$ values for A2780 and A2780cis cells.
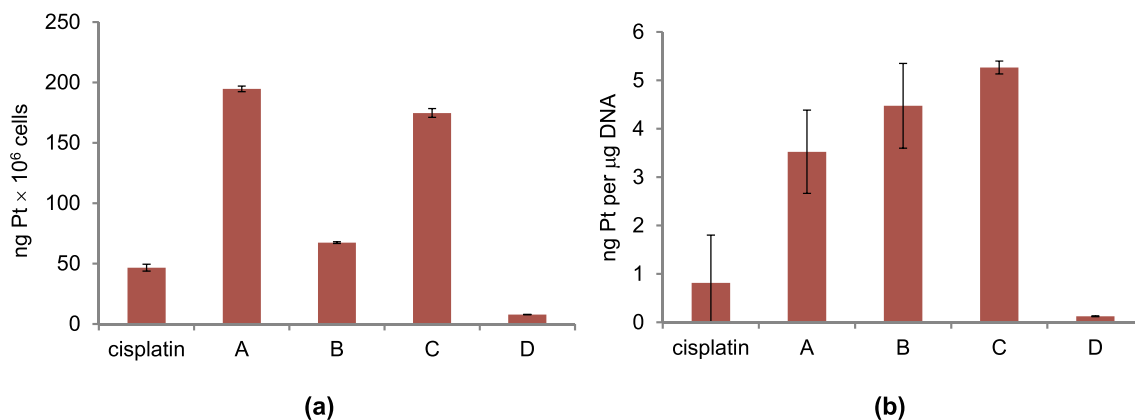
Fig. 2. (a) Cellular uptake of cisplatin and complexes **A** – **D** into A2780 cells. (b) DNA platination in A2780 cells incubated with cisplatin and complexes **A** – **D.** A2780 cells were incubated for 24 h with IC_{50} doses of the compounds (24 h concentrations according to Table 1). Error bars represent standard deviations from three independent measurements.
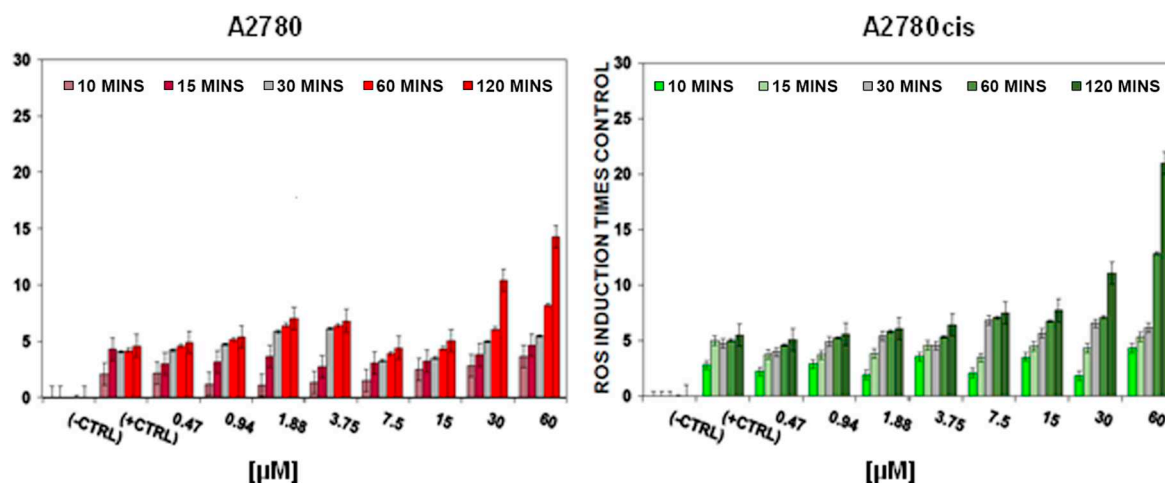

Fig. 3. Fluorescent detection of ROS using H_2DCFDA in A2780 and A2780cis cells after exposure to different concentrations of complex **C** over a period of 2 h. H_2O_2 (10 μM) was used as a positive control. Error bars represent standard deviations of three independent measurements.

diacetate (H_2DCFDA) as a peroxide-sensitive fluorescent dye (Figs. 3 and S3). A2780 cells treated with cisplatin, PBA and the Pt(IV) complexes showed a time- and concentration-dependent increase in ROS

Fig. 4. HDAC activity measured in nuclear extracts of A2780 and A2780cis cells after exposure to IC_{50} concentrations of **A** – **C**, cisplatin, PBA and SAHA. The IC_{50} concentrations of **A** – **C** and cisplatin are given in Table 1 (24 h timepoint). IC_{50} (24 h) of PBA = 1945 μM (A2780) and 2076 μM (A2780cis). IC_{50} (24 h) of SAHA = 30.2 μM (A2780) and 60.8 μM (A2780cis). Error bars represent standard deviations of three replicates.

production. However, while cisplatin, the free ligand and **A** and **D** had moderate effects only, concentrations of **C** in the IC_{50} range resulted in markedly enhanced ROS levels, comparable to those induced by the positive control H_2O_2. There were no significant differences in ROS generation on treatment with **C** between the sensitive and resistant cell line.
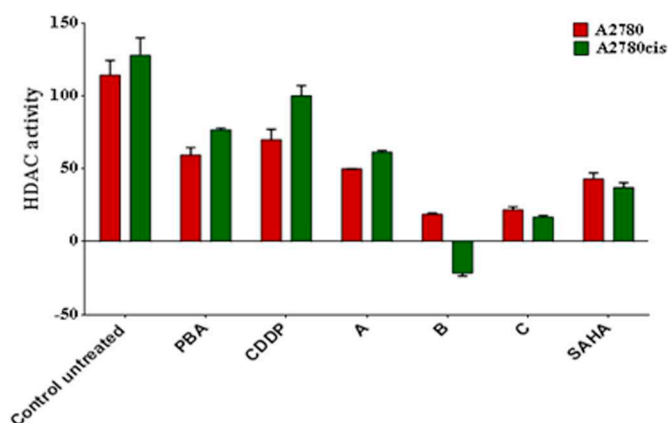
3.5. HDAC inhibition

The ability of the three most cytotoxic Pt(IV) pro-drugs to inhibit HDAC activity following activation and release of the HDACi PBA was measured in nuclear extracts of the cisplatin-sensitive and -resistant cell lines (Fig. 4). An HDAC fluorimetric activity assay was used which is the method of choice in the recent literature [20,24,27,50]. A2780 and A2780cis cells were incubated with IC_{50} doses (Tables 1, 24 h timepoint) of **A** – **C** for 24 h. Cisplatin, the free ligand PBA and the known HDAC inhibitor suberoylanilide hydroxamic acid (SAHA) were used as controls. All treated cells showed reduced HDAC activity. **B** and **C** had the strongest effect on HDAC activity and are more potent HDAC inhibitors than SAHA. The decrease in HDAC activity in A2780 and A2780cis cells treated with cisplatin is noteworthy, as this is in contrast to the study by Raveendran et al. who observed no HDAC inhibitory activity in MCF-7 cells exposed to cisplatin [27].
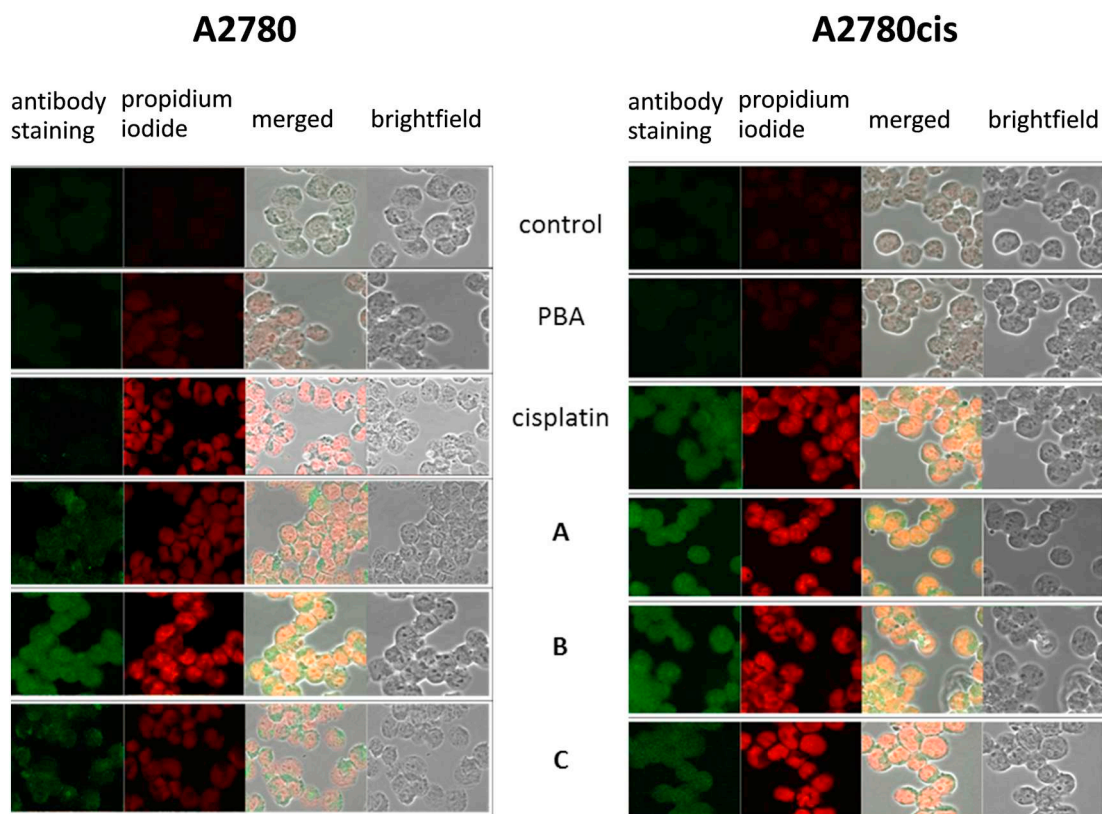
A2780   A2780cis

Fig. 5. A2780 and A2780cis cells exposed to IC_{50} concentrations of complexes **A**, **B** and **C**, cisplatin and PBA in comparison to the negative control. The IC_{50} concentrations of **A** – **C** and cisplatin are given in Table 1 (24 h timepoint). IC_{50} (24 h) of PBA = 1945 μM (A2780) and 2076 μM (A2780cis). γ-H2AX foci were visualized using primary antibody staining with fluorescent FITC secondary label. Propidium iodide was used as a nuclear counter stain.

3.6. DNA damage studies by immuno-detection of γ-H2AX foci

DNA damage induced by the coordination of cisplatin to the *N7* position of guanine bases and the formation of cisplatin-DNA cross-links triggers various cellular mechanisms such as cell cycle arrest, activation of repair mechanisms, and cell death pathways [1,51]. When the DNA damage leads to double strand breaks (DSBs), Ser-139 of the histone H2AX is rapidly phosphorylated at the site of the DSB resulting in the formation of discrete foci. The γ-H2AX foci can be detected and quantified by immunofluorescence [52–54]. The number of γ-H2AX foci is directly proportional to the DSBs and is an indicator of DNA repair efficacy. H2AX phosphorylation has been observed on treatment with cisplatin [55,56]. It is believed that the phosphorylation of H2AX plays a crucial role in the detection of DNA damage and in the activation of DNA repair pathways.

The immunofluorescence microscopy images of A2780 and A2780cis cells incubated with IC_{50} doses of complexes **A** – **C** for 24 and 48 h are depicted in Fig. 5. The formation of γ-H2AX foci is clearly visible. The images of cells treated with cisplatin and PBA are also shown for comparison.

γ-H2AX foci generation after 24 and 48 h exposure to IC_{50} concentrations of **A** – **C**, cisplatin and PBA was determined quantitatively by flow cytometry (Fig. 6). Compared to the untreated control, a significant increase in γ-H2AX foci was observed in A2780 cells treated with PBA, cisplatin, **A**, **B**, and **C** with the strongest response being elicited by **B**. Cells treated with the most potent complex **C** also show significant more DNA damage than cells treated with cisplatin. It has been reported that resistance towards cisplatin in A2780cis cells is caused by increased glutathione levels, enhanced DNA damage repair and/or enhanced DNA damage tolerance [57]. After 48 h, some decrease in γ-H2AX foci is observed in A2780 cells exposed to **B** and cisplatin indicating DNA repair. Overall, there is more DNA damage

repair in the resistant A2780cis cells compared to the sensitive cell line as expected (Fig. 6b).

3.7. Apoptosis

The induction of apoptosis in A2780 and A2780cis cells treated with **A**, **B**, **C**, cisplatin and PBA was studied using double staining with annexin V/propidium iodide (AV/PI) and flow cytometry (Fig. 7). Double staining allows for viable cells (AV-/PI-) to be distinguished in early apoptosis (AV+/PI-), late apoptosis (AV+/PI+) and necrosis (AV-/PI+). Treatment of A2780 and A2780cis cells with IC_{50} concentrations of the Pt(IV) complexes resulted in a significant percentage of late apoptotic cells after 24 h. The percentage of cells in late apoptosis are in the order **C** > **A** > cisplatin > **B** > > PBA and is similar in both cell lines. The percentage of late apoptotic cells decreases after 48 h. The observation that complex **C** leads to the highest percentage of late apoptotic cells correlates with its low IC_{50} value. Unlike cisplatin, for which a clear difference in the percentage of late apoptotic A2780 and A2780cis cells is observed, a similarly high percentage of cells of both cell lines enter the late apoptotic state on exposure to complex **C** confirming that the Pt(IV) complex is less discriminative, in line with its resistance factor value of 1.4. Apparently, the mechanism of cisplatin-resistance in A2780cis cells does not interfere with the ability of **C** to elicit its cytotoxic effect after activation and release of PBA and cisplatin. Cellular responses to ROS and apoptosis are linked to the mitochondria which are involved in the resistance mechanism of A2780cis cells [58]. A recent in-depth mechanistic study has shown that the apoptosis and mitochondria-related gene expression profiles of A2780cis cells after exposure to Cu diimine complexes contrast with the response of A2780 cells [59]. Similar investigations using the Pt PBA complexes will be of interest for future work.
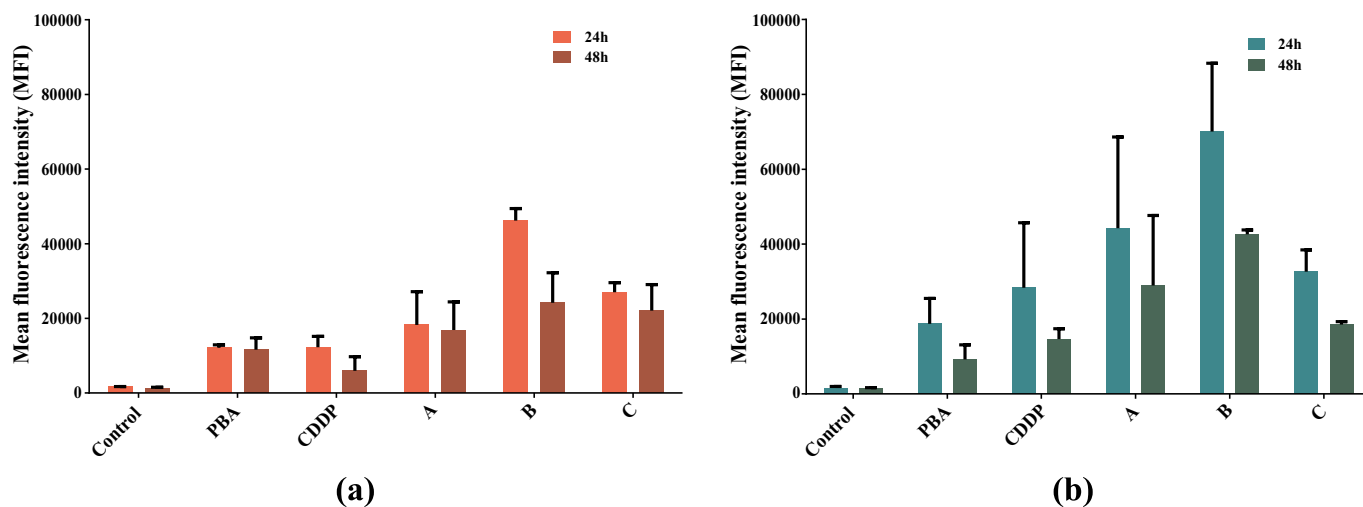
Fig. 6. Immuno-detection of γ-H2AX foci post exposures in (a) A2780 and (b) A2780cis cells treated with IC$_{50}$ doses of complexes **A – C**, cisplatin and PBA. The IC$_{50}$ concentrations of **A – C** and cisplatin are given in Table 1 (24 h timepoint). IC$_{50}$ (24 h) of PBA = 1945 μM (A2780) and 2076 μM (A2780cis). Error bars represent standard deviations of three independent measurements.
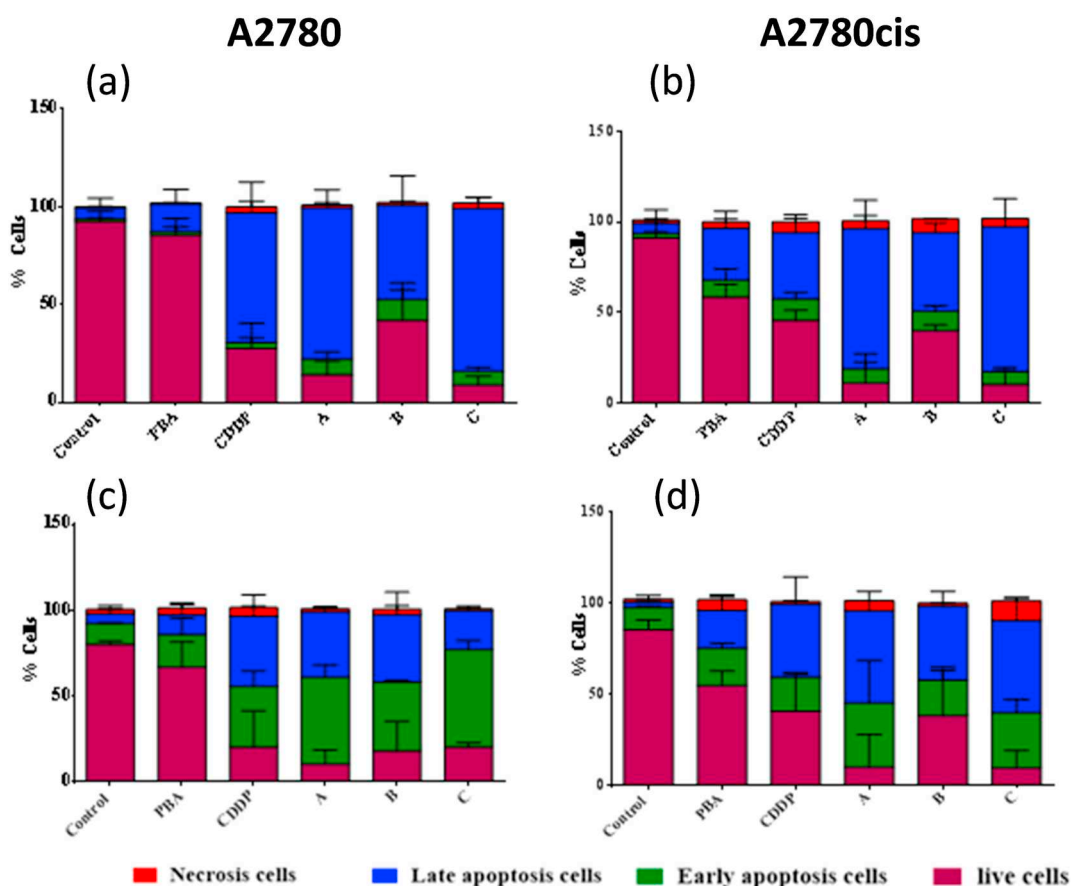

Fig. 7. Annexin V/PI staining and flow cytometry analysis of A2780 and A2780cis cells after 24 h (a, b) and after 48 h (c, d) exposure to IC$_{50}$ concentrations of **A, B, C**, cisplatin and PBA. The IC$_{50}$ concentrations of **A – C** and cisplatin are given in Table 1 (24 h timepoint). IC$_{50}$ (24 h) of PBA = 1945 μM (A2780) and 2076 μM (A2780cis). Error bars represent standard deviations of three independent measurements.

4. Conclusions

The monosubstituted complex *cis,cis,trans*-[Pt(NH$_3$)$_2$Cl$_2$(PBA)(OH)], the symmetrically disubstituted complex *cis,cis,trans*-[Pt(NH$_3$)$_2$Cl$_2$(PBA)$_2$] and the unsymmetrically disubstituted complex *cis,cis,trans*-[Pt(NH$_3$)$_2$Cl$_2$(PBA)(Bz)] overcome cisplatin resistance, are more cytotoxic in

A2780 and A2780cis ovarian cancer cells than cisplatin and induce cell death pathways leading to apoptosis in both cell lines.

While our study confirms that the three Pt(IV) complexes interact with their intended targets, DNA and HDAC, it has to be kept in mind that their mode(s) of action may be more complex. PBA is also known to activate transcription factors that upregulate genes for lipid

metabolizing enzymes [60] and to reverse the Warburg effect by inhibiting pyruvate dehydrogenase kinase [61]. The suggestion that many Pt(IV) complexes with a bioactive axial ligand designed as dual-action pro-drugs may in fact be multi-action pro-drugs was discussed in a recent review article [62]. The ROS data seem to support a multimodal mechanism for the PBA complexes. ROS play a role in the activation of signalling pathways and transcription factors that induce cell death processes including apoptosis. At concentrations close to its IC_{50} value the most cytotoxic complex **C** leads to markedly increased cellular ROS levels which can mediate apoptosis independent of DNA damage. Consistently, the γ-H2AX foci generation data confirm that the Pt(IV) PBA complexes kill cancer cells only to a certain extent by DNA damage and that DNA damage is only one of their cytotoxic effects.

In summary, *cis,cis,trans*-[Pt(NH$_3$)$_2$Cl$_2$(PBA)(OH)], *cis,cis,trans*-[Pt(NH$_3$)$_2$Cl$_2$(PBA)$_2$] and *cis,cis,trans*-[Pt(NH$_3$)$_2$Cl$_2$(PBA)(Bz)] are potent cytotoxins that act *via* multimodal mechanisms involving DNA damage *via* γ-H2AX foci production and cell death mechanisms independent of cisplatin resistance.

Declaration of competing interests

The authors declare that they have no known competing financial interests or personal relationships that could have appeared to influence the work reported in this paper.

Acknowledgements

Appendix A. Supplementary data

Supplementary data to this article can be found online at https://doi.org/10.1016/j.jinorgbio.2020.111125.

References

[1] T.C. Johnstone, K. Suntharalingam, S.J. Lippard, The next generation of platinum drugs: targeted Pt(II) agents, nanoparticle delivery, and Pt(IV) prodrugs, Chem. Rev. 116 (2016) 3436–3486, https://doi.org/10.1021/acs.chemrev.5b00597.

[2] K. Kohno, T. Uchiumi, I. Niina, T. Wakasugi, T. Igarashi, Y. Momii, T. Yoshida, K. Matsuo, N. Miyamoto, H. Izumi, Transcription factors and drug resistance, Eur. J. Cancer 41 (2005) 2577–2586, https://doi.org/10.1016/j.ejca.2005.08.007.

[3] T. Torigoe, H. Izumi, H. Ishiguchi, Y. Yoshida, M. Tanabe, T. Yoshida, T. Igarashi, I. Niina, T. Wakasugi, T. Imaizumi, Y. Momii, M. Kuwano, K. Kohno, Cisplatin resistance and transcription factors, Curr. Med. Chem. Anti-Cancer Agents 5 (2005) 15–27, https://doi.org/10.2174/1568011053352587.

[4] G. Housman, S. Byler, S. Heerboth, K. Lapinska, M. Longacre, N. Snyder, S. Sarkar, Drug resistance in cancer: an overview, Cancers 6 (2014) 1769–1792, https://doi.org/10.3390/cancers6031769.

[5] D.-W. Shen, L.M. Pouliot, M.D. Hall, M.M. Gottesman, Cisplatin resistance: a cellular self-defense mechanism resulting from multiple epigenetic and genetic changes, Pharmacol. Rev. 64 (2012) 706–721, https://doi.org/10.1124/pr.111.005637.

[6] T. Kouzarides, Chromatin modifications and their function, Cell 128 (2007) 693–705, https://doi.org/10.1016/j.cell.2007.02.005.

[7] B.D. Strahl, C.D. Allis, The language of covalent histone modifications, Nature 403 (2000) 41–45, https://doi.org/10.1038/47412.

[8] R. Juergens, J. Wrangle, F. Vendetti, S.C. Murphy, M. Zhao, B. Coleman, R. Sebree, K. Rodgers, C.M. Hooker, N. Franco, B. Lee, S. Tsai, I. Espinoza Delgado, M.A. Rudek, S.A. Belinsky, J.G. Herman, S.B. Baylin, M.V. Brock, C.M. Rudin, Combination epigenetic therapy has efficacy in patients with refractory advanced non-small cell lung cancer, Cancer Discov 1 (2011) 598–607, https://doi.org/10.1158/2159-8290.CD-11-0214.

[9] M.J. Lee, Y.S. Kim, S. Kummar, G. Giaccone, J.B. Trepel, Histone deacetylase inhibitors in cancer therapy, Curr. Opin. Oncol. 29 (2008) 639–649, https://doi.org/10.1097/cco.0b013e3283127095.

[10] G.R. Leggatt, B. Gabrielli, Histone deacetylase inhibitors in the generation of the anti-tumour immune response, Immunol. Cell Biol. 90 (2011) 33–38, https://doi.org/10.1038/icb.2011.94.

[11] B.S. Mann, J.R. Johnson, M.H. Cohen, R. Justice, R. Pazdur, FDA approval summary: Vorinostat for treatment of advanced primary cutaneous T-cell lymphoma, Oncologist 12 (2007) 1247–1252, https://doi.org/10.1634/theoncologist.12-10-1247.

[12] H.V. Diyabalanage, M.L. Granda, J.M. Hooker, Combination therapy: histone deacetylase inhibitors and platinum-based chemotherapeutics for cancer, Cancer Lett. 329 (2013) 1–8, https://doi.org/10.1016/j.canlet.2012.09.018.

[13] W.J. Huang, Y.A. Tang, M.Y. Chen, Y.J. Wang, F.H. Hu, T.W. Wang, S.W. Chao, H.W. Chiu, L. Yeh, H.Y. Chang, H.F. Juan, P. Lin, Y.C. Wang, A histone deacetylase inhibitor YCW1 with antitumor and antimetastasis properties enhances cisplatin activity against non-small cell lung cancer in preclinical studies, Cancer Lett. 346 (2014) 84–93, https://doi.org/10.1016/j.canlet.2013.12.016.

[14] K.L. Jin, Y. Park, E.J. Noh, K.L. Hoe, J.H. Lee, J.H. Kim, J.H. Nam, The effect of combined treatment with cisplatin and histone deacetylase inhibitors on HeLa cells, J. Gynecol. Oncol. 21 (2010) 262–268, https://doi.org/10.3802/jgo.2010.21.4.262.

[15] K.K.W. To, W.S. Tong, L.W. Fu, Reversal of platinum drug resistance by the histone deacetylase inhibitor belinostat, Lung Cancer 103 (2017) 58–65, https://doi.org/10.1016/j.lungcan.2016.11.019.

[16] X. Zhang, M. Yashiro, J. Ren, K. Hirakawa, Histone deacetylase inhibitor, trichostatin a, increases the chemosensitivity of anticancer drugs in gastric cancer cell lines, Oncol. Rep. 16 (2006) 563–568.

[17] E. Cacan, M.W. Ali, N.H. Boyd, S.B. Hooks, S.F. Greer, Inhibition of HDAC1 and DNMT1 modulate RGS10 expression and decrease ovarian cancer chemoresistance, PLoS One 9 (2014) e87455, , https://doi.org/10.1371/journal.pone.0087455.

[18] D.M. Griffith, B. Duff, K.Y. Suponitsky, K. Kavanagh, M.P. Morgan, D. Egan, C.J. Marmion, Novel *trans*-platinum complexes of the histone deacetylase inhibitor valproic acid; synthesis, *in vitro* cytotoxicity and mutagenicity, J. Inorg. Biochem. 105 (2011) 793–799, https://doi.org/10.1016/j.jinorgbio.2011.03.001.

[19] V. Brabec, D.M. Griffith, A. Kisova, H. Kostrhunova, L. Zerzankova, C.J. Marmion, J. Kasparkova, Valuable insight into the anticancer activity of the platinum-histone deacetylase inhibitor conjugate, cis-[Pt(NH$_3$)$_2$malSAHA$_{-2H}$], Mol. Pharm. 9 (2012) 1990–1999, https://doi.org/10.1021/mp300038f.

[20] D. Griffith, M.P. Morgan, C.J. Marmion, A novel anti-cancer bifunctional platinum drug candidate with dual DNA binding and histone deacetylase inhibitory activity, Chem. Commun. (2009) 6735–6737, https://doi.org/10.1039/b916715c.

[21] J.P. Parker, H. Nimir, D.M. Griffith, B. Duff, A.J. Chubb, M.P. Brennan, M.P. Morgan, D.A. Egan, C.J. Marmion, A novel platinum complex of the histone deacetylase inhibitor belinostat: rational design, development and in vitro cytotoxicity, J. Inorg. Biochem. 124 (2013) 70–77, https://doi.org/10.1016/j.jinorgbio.2013.03.011.

[22] J. Kasparkova, H. Kostrhunova, O. Novakova, R. Krikavova, J. Vanco, Z. Travnicek, V. Brabec, A photoactivatable platinum(IV) complex targeting genomic DNA and histone deacetylases, Angew. Chem. Int. Ed. 54 (2015) 14478–14482, https://doi.org/10.1002/anie.201506533.

[23] B.W.J. Harper, E. Petruzzella, R. Sirota, F.F. Faccioli, J.R. Aldrich-Wright, V. Gandin, D. Gibson, Synthesis, characterization and in vitro and in vivo anticancer activity of Pt(IV) derivatives of [Pt(1S,2S-DACH)(5,6-dimethyl-1,10-phenanthroline)], Dalton Trans. 46 (2017) 7005–7019, https://doi.org/10.1039/c7dt01054k.

[24] H. Kostrhunova, Z. Zajac, V. Novohradsky, J. Kasparkova, J. Malina, J.R. Aldrich-Wright, E. Petruzzella, R. Sirota, D. Gibson, V. Brabec, A subset of new platinum antitumor agents kills cells by a multimodal mechanism of action also involving changes in the organization of the microtubule cytoskeleton, J. Med. Chem. 62 (2019) 5176–5190, https://doi.org/10.1021/acs.jmedchem.9b00489.

[25] V. Novohradsky, L. Zerzankova, J. Stepankova, O. Vrana, R. Raveendran, D. Gibson, J. Kasparkova, V. Brabec, Antitumor platinum(IV) derivatives of oxaliplatin with axial valproato ligands, J. Inorg. Biochem. 140 (2014) 72–79, https://doi.org/10.1016/j.jinorgbio.2014.07.004.

[26] V. Novohradsky, L. Zerzankova, J. Stepankova, O. Vrana, R. Raveendran, D. Gibson, J. Kasparkova, V. Brabec, New insights into the molecular and epigenetic effects of antitumor Pt(IV)-valproic acid conjugates in human ovarian cancer cells, Biochem. Pharmacol. 95 (2015) 133–144, https://doi.org/10.1016/j.bcp.2015.04.003.

[27] R. Raveendran, J.P. Braude, E. Wexselblatt, V. Novohradsky, O. Stuchlikova, V. Brabec, V. Gandin, D. Gibson, Pt(IV) derivatives of cisplatin and oxaliplatin with phenylbutyrate axial ligands are potent cytotoxic agents that act by several mechanisms of action, Chem. Sci. 7 (2016) 2381–2391, https://doi.org/10.1039/C5SC04205D.

[28] M. Alessio, I. Zanellato, I. Bonarrigo, E. Gabano, M. Ravera, D. Osella, Antiproliferative activity of Pt(IV)-bis(carboxylato) conjugates on malignant pleural mesothelioma cells, J. Inorg. Biochem. 129 (2013) 52–57, https://doi.org/10.1016/j.jinorgbio.2013.09.003.

[29] J. Yang, X. Sun, W. Mao, M. Sui, J. Tang, Y. Shen, Conjugate of Pt(IV)–histone deacetylase inhibitor as a prodrug for cancer chemotherapy, Mol. Pharm. 9 (2012) 2793–2800, https://doi.org/10.1021/mp200597r.

[30] H. Kostrhunova, E. Petruzzella, D. Gibson, J. Kasparkova, V. Brabec, An anticancer Pt^{IV} prodrug that acts by mechanisms involving DNA damage and different epigenetic effects, Chem. Eur. J. 25 (2019) 5235–5245, https://doi.org/10.1002/chem.201805626.

[31] A.R.Z. Almotairy, V. Gandin, L. Morrison, C. Marzano, D. Montagner, A. Erxleben, Antitumor platinum(IV) derivatives of carboplatin and the histone deacetylase inhibitor 4-phenylbutyric acid, J. Inorg. Biochem. 177 (2017) 1–7, https://doi.org/10.1016/j.jinorgbio.2017.09.009.

[32] M. Crespo Alonso, A. Rigoldi, A. Ibba, L. Zicca, P. Deplano, M.L. Mercuri, P. Cocco, A. Serpe, A simple, sensitive analytical method for platinum trace determination in human urine, Microchem. J. 122 (2015) 1–4, https://doi.org/10.1016/j.microc.2015.03.016.

[33] J.G. Morrison, P. White, S. McDougall, J.W. Firth, S.G. Woolfrey, M.A. Graham, D. Greenslade, Validation of a highly sensitive ICP-MS method for the determination of platinum in biofluids: application to clinical pharmacokinetic studies with oxaliplatin, J. Pharm. Biomed. Anal. 24 (2000) 1–10, https://doi.org/10.1016/

s0731-7085(00)00377-0.

[34] N.I. Ward, L.M. Dudding, Platinum emissions and levels in motorway dust samples: influence of traffic characteristics, Sci. Total Environ. 334 (2004) 457–463, https://doi.org/10.1016/j.scitotenv.2004.04.049.

[35] J.D. Whiteley, F. Murray, Determination of selected actinides (U, Pu and Am) in Belarus soils using high resolution inductively coupled plasma mass and gamma spectrometry, Geochemistry: Exploration, Environment, Analysis 5 (2005) 3–10, https://doi.org/10.1144/1467-7873/03-035.

[36] T. Mosmann, Rapid colorimetric assay for cellular growth and survival: application to proliferation and cytotoxicity assays, J. Immunol. Methods 65 (1983) 55–63, https://doi.org/10.1016/0022-1759(83)90303-4.

[37] E. Wexselblatt, D. Gibson, What do we know about the reduction of Pt(IV) pro-drugs? J. Inorg. Biochem. 117 (2012) 220–229, https://doi.org/10.1016/j.jinorgbio.2012.06.013.

[38] J.Z. Zhang, E. Wexselblatt, T.W. Hambley, D. Gibson, Pt(IV) analogs of oxaliplatin that do not follow the expected correlation between electrochemical reduction potential and rate of reduction by ascorbate, Chem. Comm. 48 (2012) 847–849, https://doi.org/10.1039/c1cc16647f.

[39] N. Graf, S.J. Lippard, Redox activation of metal-based prodrugs as a strategy for drug delivery, Adv. Drug Del. Rev. 64 (2012) 993–1004, https://doi.org/10.1016/j.addr.2012.01.007.

[40] U. Ben-David, B. Siranosian, G. Ha, H. Tang, Y. Oren, K. Hinohara, C.A. Strathdee, J. Dempster, N.J. Lyons, R. Burns, A. Nag, G. Kugener, B. Cimini, P. Tsvetkov, Y.E. Maruvka, R. O'Rourke, A. Garrity, A.A. Tubelli, P. Bandopadhayay, A. Tsherniak, F. Vazquez, B. Wong, C. Birger, M. Ghandi, A.R. Thorner, J.A. Bittker, M. Meyerson, G. Getz, R. Beroukhim, T.R. Golub, Genetic and transcriptional evolution alters cancer cell line drug response, Nature 560 (2018) 325–330, https://doi.org/10.1038/s41586-018-0409-3.

[41] K.A. Strait, C.T. Warnick, C.D. Ford, B. Dabbas, E.H. Hammond, S.J. Ilstrup, Histone deacetylase inhibitors induce G2-checkpoint arrest and apoptosis in cisplatinum-resistant ovarian cancer cells associated with overexpression of the Bcl-2-related protein Bad, Mol. Cancer Ther. 4 (2005) 603–611, https://doi.org/10.1158/1535-7163.MCT-04-0107.

[42] S.L. Hulin-Curtis, J.A. Davies, R. Jones, E. Hudson, L. Hanna, J.D. Chester, A.L. Parker, Histone deacetylase inhibitor trichostatin A sensitises cisplatin-re-sistant ovarian cancer cells to oncolytic adenovirus, Oncotarget 29 (2018) 26328–26341, https://doi.org/10.18632/oncotarget.25242.

[43] X. Jin, Y. Fang, Y. Hu, J. Chen, W. Liu, G. Chen, M. Gong, P. Wu, T. Zhu, S. Wang, J. Zhou, H. Wang, D. Ma, K. Li, Synergistic activity of the histone deacetylase in-hibitor trichostatin A and the proteasome inhibitor PS-341 against taxane-resistant ovarian cancer cell lines, Oncol. Lett. 13 (2017) 4619–4626, https://doi.org/10.3892/ol.2017.6032.

[44] D. Tolan, V. Gandin, L. Morrison, A. El-Nahas, C. Marzano, D. Montagner, A. Erxleben, Oxidative stress induced by Pt(IV) pro-drugs based on the cisplatin scaffold and indole carboxylic acids in axial position, Sci. Rep. 6 (2016) 29367, , https://doi.org/10.1038/srep29367.

[45] J. Zajac, H. Kostrhunova, V. Novohradsky, O. Vrana, R. Raveendran, D. Gibson, J. Kasparkova, V. Brabec, Potentiation of mitochondrial dysfunction in tumor cells by conjugates of metabolic modulator dichloroacetate with a Pt(IV) derivative of oxaliplatin, J. Inorg. Biochem. 156 (2016) 89–97, https://doi.org/10.1016/j.jinorgbio.2015.12.003.

[46] V. Pichler, S. Göschl, E. Schreiber-Brynzak, M.A. Jakupec, M. Galanski, B.K. Keppler, Influence of reducing agents on the cytotoxic activity of platinum(IV) complexes: induction of G 2/M arrest, apoptosis and oxidative stress in A2780 and cisplatin resistant A2780cis cell lines, Metallomics 7 (2015) 1078–1090, https://doi.org/10.1039/c5mt00116a.

[47] G.N. Kaluđerović, S.A. Mijatović, B.B. Zmejkovski, M.Z. Bulatović, S. Gómez-Ruiz, M.K. Mojić, D. Steinborn, D.M. Miljković, H. Schmidt, S.D. Stošić-Grujičić, T.J. Sabo, D.D. Maksimović-Ivanić, Platinum(II/IV) complexes containing ethyle-nediamine-N,N-di-2/3-propionate ester ligands induced caspase-dependent apop-tosis in cisplatin-resistant colon cancer cells, Metallomics 4 (2002) 979–987, https://doi.org/10.1039/c2mt20058a.

[48] U. Jungwirth, C.R. Kowol, B.K. Keppler, C.G. Hartinger, W. Berger, P. Heffeter, Anticancer activity of metal complexes: involvement of redox processes, Antioxid. Redox Signal. 15 (2011) 1085–1127, https://doi.org/10.1089/ars.2010.3663.

[49] H. Pelicano, D. Carney, P. Huang, ROS stress in cancer cells and therapeutic im-plications, Drug Resist. Updat. 7 (2004) 97–100, https://doi.org/10.1016/j.drup.2004.01.004.

[50] E. Petruzzella, R. Sirota, I. Solazzo, V. Gandin, D. Gibson, Triple action Pt(IV) de-rivatives of cisplatin: a new class of potent anticancer agents that overcome re-sistance, Chem. Sci. 9 (2018) 4299–4307, https://doi.org/10.1039/C8SC00428E.

[51] D. Wang, S.J. Lippard, Cellular processing of platinum anticancer drugs, Nat. Rev. Drug Discov. 4 (2005) 307–320, https://doi.org/10.1038/nrd1691.

[52] T. Ohnishi, E. Mori, A. Takahashi, DNA double-strand breaks: their production, recognition, and repair in eukaryotes, Mutat. Res. 669 (2009) 8–12, https://doi.org/10.1016/j.mrfmmm.2009.06.010.

[53] M. Podhorecka, A. Skladanowski, P. Bozko, H2AX phosphorylation: its role in DNA damage response and cancer therapy, J. Nucleic Acids 2010 (2010) 920161, , https://doi.org/10.4061/2010/920161.

[54] A. Takahashi, T. Ohnishi, Does gammaH2AX foci formation depend on the presence of DNA double strand breaks? Cancer Lett. 229 (2005) 171–179, https://doi.org/10.1016/j.canlet.2005.07.016.

[55] X. Huang, M. Okafuji, F. Traganos, E. Luther, E. Holden, Z. Darzynkiewicz, Assessment of histone H2AX phosphorylation induced by DNA topoisomerase I and II inhibitors topotecan and mitoxantrone and by the DNA cross-linking agent cis-platin, Cytometry A 58 (2004) 99–110, https://doi.org/10.1002/cyto.a.20018.

[56] A. Pines A.C.D. Kelstrup, M.G. Vrouwe, J.C. Puigvert, D. Typas, B. Misovic, A. de Groot, L. von Stechow, B. van de Water, E.H.J. Danen, H. Vrieling, L.H.F. Mullenders, J. Olsen, V.V. Jesper, Global phosphoproteome profiling reveals un-anticipated networks responsive to cisplatin treatment of embryonic stem cells, Mol. Cell. Biol. 31 (2011) 4964–4977, doi:https://doi.org/10.1128/MCB.05258-11.

[57] B.C. Behrens, T.C. Hamilton, H. Masuda, K.R. Grotzinger, J. Whang-Peng, K.G. Louie, T. Knutsen, W.M. McKoy, R. Young, R.F. Ozols, Characterization of a cis-diamminedichloro-platinum(II)-resistant human ovarian cancer cell line and its use in evaluation of platinum analogues, Cancer Res. 47 (1987) 414–418.

[58] M. Redza-Dutordoir, D.A. Averill-Bates, Activation of apoptosis signalling pathways by reactive oxygen species, Biochim. Biophys. Acta, Mol. Cell Res. 1863 (2016) 2977–2992, https://doi.org/10.1016/j.bbamcr.2016.09.012.

[59] G. Rochford, Z. Molphy, K. Kavanagh, M. McCann, M. Devereux, A. Kellett, O. Howe, Cu(II) phenanthroline–phenazine complexes dysregulate mitochondrial function and stimulate apoptosis, Metallomics 12 (2020) 65–78, https://doi.org/10.1039/c9mt00187e.

[60] T. Pineau, W.R. Hudgins, L. Liu, L.C. Chen, T. Sher, F.J. Gonzalez, D. Samid, Activation of a human peroxisome proliferator-activated receptor by the antitumor agent phenylacetate and its analogs, Biochem. Pharmacol. 52 (1996) 659–667, https://doi.org/10.1016/0006-2952(96)00340-1.

[61] R. Ferriero, C. Iannuzzi, G. Manco, N. Brunetti-Pierri, Differential inhibition of PDKs by phenylbutyrate and enhancement of pyruvate dehydrogenase complex activity by combination with dichloroacetate, J. Inherit. Metab. Dis. 38 (2015) 895–904, https://doi.org/10.1007/s10545-014-9808-2.

[62] D. Gibson, Multi-action Pt(IV) anticancer agents; do we understand how they work? J. Inorg. Biochem. 191 (2019) 77–84, https://doi.org/10.1016/j.jinorgbio.2018.11.008.